Available online at www.sciencedirect.com
SCIENCE DIRECT
Tetrahedron
Tetrahedron 60 (2004) 10029–10038

Double versus single helical structures of oligopyridine-dicarboxamide strands. Part 1: Effect of oligomer length

Hua Jiang, Victor Maurizot and Ivan Huc*

Institut Européen de Chimie et Biologie, 2 rue Robert Escarpit, 33607 Pessac, France

Received 25 June 2004; revised 12 July 2004; accepted 28 July 2004

Available online 11 September 2004

Abstract—Oligoamides of 2,6-diaminopyridine and 2,6-pyridinedicarboxylic acid were previously shown to fold into single helical monomers and to hybridize into double helical dimers. A new series of these oligomers comprising 5 to 15 pyridine units, 4-decyloxy residues, and benzylcarbamate end groups were synthesized using a new convergent scheme that involves an early disymmetrization of the diamine and of the diacid. The hybridization of these compounds into double helices was studied by ^{1}H NMR spectroscopy in chloroform solutions at various temperatures. Somewhat unexpectedly, these studies revealed that dimerization increases with oligomer length up to a certain point, and then decreases down to undetectable levels for the longest strands. NMR studies show that both double helices and single helices become more stable when strand length increases. The measured values of enthalpy and entropy of hybridization for oligomers of various length show that the enthalpic gain constantly decreases with strand length. This can be interpreted as being the result of an increasing enthalpic price of the spring-like extension that the strand undergoes upon hybridization as its length increases. On the other hand, the entropic loss of hybridization also constantly decreases with strand length. Presumably, the helical preorganization of the monomers increases with strand length, which allows the longer strands to hybridize with a minimal loss of motional freedom, that is to say at a low entropic price. The competiton between these two factors results in a maximum of hybridization for the strands having an intermediate length.

1. Introduction

In recent years, much effort has been devoted to the design and characterization of artificial oligomers capable of pairing into duplexes through multiple cooperative and selective interactions.[1] These structures are useful tools for the orchestration of self-assembly and self-organization at a nanometer level. They also give new insights on the functions of strand pairing as it occurs in biological systems as, for example, the duplication of information coded in a molecular strand through the template directed growth of a complementary strand.

Artificial molecular duplexes may be stabilized by (self)-complementary hydrogen bond arrays. They can be directly inspired by natural hybridization motifs as, for example, the pairing of nucleobases[1–3] or the double stranded β-barrel of the bacterial peptide Gramicidin D[4] which both give rise to double helical architectures. Several non-natural hydrogen bond arrays have also been designed.[1,5–12] The three dimensional structures of these molecular duplexes have not always been characterized in detail but the two strands are most often supposed to adopt a ladder (or zipper) like linear conformation. Another common way to direct the assembly of a molecular duplex or triplex is to use metal ions[1,13] or anions[14] as templates around which two or three strands wind upon establishing selective interactions. This leads to doubly or triply stranded helical architectures termed helicates. Less commonly, artificial duplexes based on inter-strand aromatic–aromatic interactions have also been described.[15]

Oligoamide strands derived from 2,6-diaminopyridine and 2,6-pyridinedicarboxylic acid (AOA's) belong to the wider class of aromatic oligoamides which adopt well-defined folded conformations.[16–20] AOA's self-organize into single helical conformers stabilized by both attractive and repulsive interactions involving either the amide hydrogen or oxygen on the one hand, and the adjacent pyridine nitrogen and protons on the other hand (Fig. 1). Additionally, the helices gain stability from intramolecular aromatic–aromatic interaction.[16,18] Remarkably, in non polar solvents, the single helices of AOA's can extend like springs and reversibly assemble, giving rise to double-helical dimeric complexes (Fig. 1).[19,20] These artificial molecular

Keywords: Helical structures; Molecular recognition; Pi interactions; Self-assembly.
* Corresponding author. Tel.: +33-54000-2219; fax: +33-54000-3009; e-mail: i.huc@iecb.u-bordeaux.fr

0040–4020/$ - see front matter © 2004 Elsevier Ltd. All rights reserved.
doi:10.1016/j.tet.2004.07.078

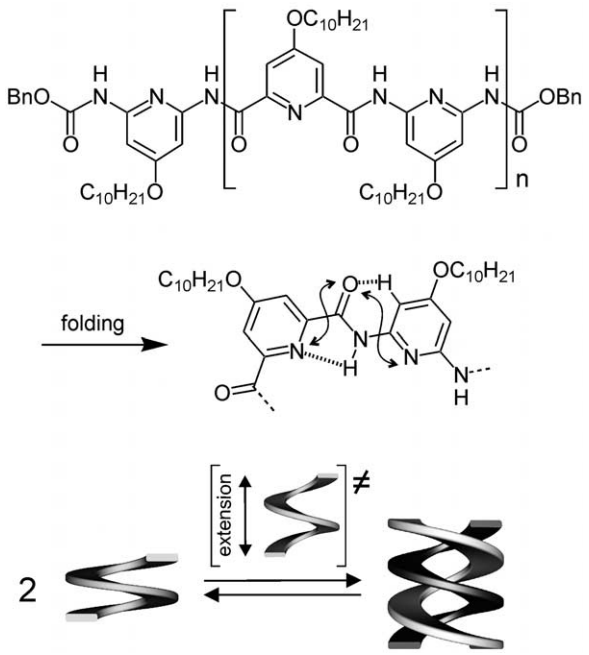

Figure 1. Intramolecular hydrogen bonds involved in helical conformations of pyridine oligoamides and schematic representation of single helix/double helix equilibrium implying a spring like extension/compression of the strands. The double headed arrows indicate electrostatic repulsions.

duplexes represent an original example of double helices stabilized by direct interactions between the strands following a non-natural hybridization motif. In contrast with helicates,[13,14] their winding into double helices takes place without the help of a template. The double helices of AOA's involve extensive interstrand aromatic–aromatic interactions,[19,20] unlike natural double helices, for example, DNA or Gramicidine D, and their synthetic analogs,[2–4] which are based on interstrand hydrogen bonding.

Short double helices of AOA's comprising five or seven pyridine units per strand were previously characterized in solution by ^{1}H NMR spectroscopy, in the solid state by X-ray crystallography, and by molecular modeling studies.[19,20] In this report, we present the synthesis of much longer chloroform soluble strands and show that, somewhat counter intuitively, dimerization of AOA's into double helices increases with strand length to reach a maximum and then decreases down to undetectable levels for the longest strands. This can be interpreted as being the result of two competing factors: the enthalpic gain of hybridization decreases as strand length increases, but the entropic loss of hybridization also decreases as strand length increases.

2. Results and discussion

2.1. Synthesis

A series of oligomers was prepared according to a new scheme that avoids the low yielding late disymmetrization steps involved in the previous syntheses.[18,19] Using a convergent strategy, we could produce molecular strands up to twice as long as the longest chloroform soluble oligomers that we described previously. In the following, oligomers are labeled according to the number of pyridine rings that they contain. Thus, diester **1a** and diamine **1b** are efficiently disymmetrized at an early stage of the synthesis (Scheme 1). Diester **1a** is monosaponified with 1 equiv of NaOH in 85% yield. Diamine **1b** is deprotonated and converted to its mono-amine mono-benzylcarbamate **1d** in 67% yield. This compound can be coupled to 4-decyloxy-2,6-pyridine dicarbonyl chloride or to the acid chloride of **1c** to give protected diamine **3a** and protected aminoacid **2a**, respectively. These products are quantitatively deprotected at the N terminus using hydrogenation on Pd/C, and at the C terminus using NaOH. Trimer **3b** can also be prepared by directly reacting the anion of diamine **1b** and diester **1a**. Cycles of deprotection, activation via the acid chloride and coupling, allow to convert **2a** into tetrameric strand **4b** and hexameric strand **6b** (Scheme 2). Finally, two dimeric, tetrameric or hexameric acid chloride units can be attached to a monomeric or trimeric diamine core to give oligomers **5**–**15** in moderate yield (Scheme 3).

2.2. Dimerization constants as a function of strand length

The alkoxy chains in position 4 of the pyridines diverge from the helices and confer all oligomers with high solubility in chlorinated, aromatic, and alkane solvents. The ability of strands **5**–**15** to dimerize was investigated in $CDCl_3$ (Fig. 2). As shown by the ^{1}H NMR spectra, single and double helices undergo slow exchange and give rise to different signals. The coalescence between these signals is not reached below the boiling point of chloroform for all these compounds except **5** for which most of the signals coalesce between 25 and 35 °C.

The NMR signals can easily be assigned to the single and double helices according to the variation of their relative intensity upon changing temperature or concentration: the proportion of single helix increases upon heating and upon diluting. The assignment of the signals can also be deduced from the fact that single and double helices do not have the

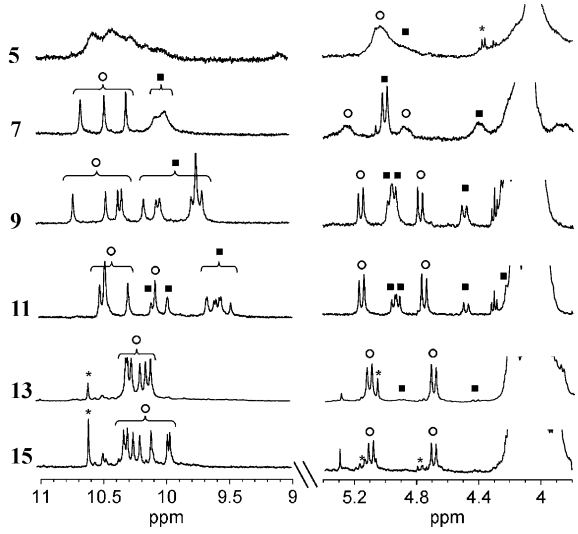

Figure 2. Part of the ^{1}H 400 MHz NMR spectra of compound **5**–**15** at 25 °C, C=1 mM in $CDCl_3$, showing the resonances of the amides (11–9 ppm) and the resonnances of the benzylic methylenes (5.4–4.4 ppm). Signals assigned to single and double helices, and to impurities[21] are labelled by circles, squares, and asterisks respectively.

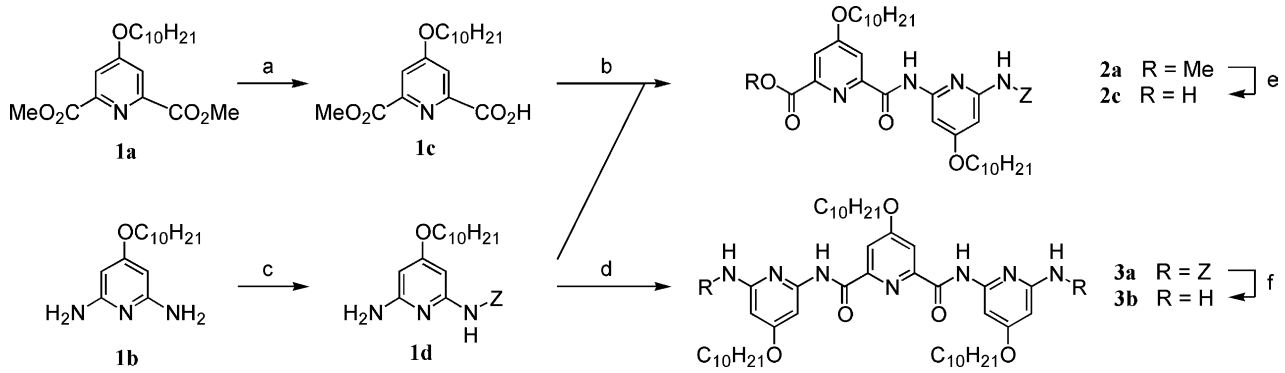

Scheme 1. Reagents and conditions: (a) MeOH–dioxane, 0 °C, NaOH (1 equiv), 85% yield; (b) $SOCl_2$, reflux, then **1d**, toluene, iPr$_2$EtN, RT, 90% yield; (c) THF, −78 °C, n-BuLi (1 equiv), $ClCO_2Bn$ (1 equiv), 67% yield; (d) toluene, 4-decyloxypyridine 2,6-dicarbonylchloride (0.45 equiv), iPr$_2$EtN, RT, 83% yield; (e) H_2O–dioxane, 25 °C, NaOH (2 equiv), quant. yield; (f) ethyl acetate/AcOH, RT, H_2/Pd–C, quant. yield.

same symmetry. The single helices possess a C_2 symmetry axis perpendicular to the helical axis. Each signal is therefore degenerate and corresponds to the two protons occupying equivalent positions at each end of the strand. This symmetry is lost in the double helices in which the two strands are equivalent, but the extremities of each strand are in different environments. A double helix thus gives rise to twice as many signals as the corresponding single helix (see the spectra of **9**–**15** in Fig. 2). However, this only holds below a certain temperature. Sliding motions within the double helix allow the exchange between the different environments of each strand. When this becomes fast on the NMR timescale, a coalescence takes place and the NMR spectrum of an on-average C_2 symmetrical double helix is seen (see the spectrum of **7** in Fig. 2).

The considerable size of these synthetic double helices should be emphasized. Dimer $(\mathbf{13})_2$, for example, spans over three double-helical turns and is more than 2 nm long with a molecular weigh of 7700 g mol^{-1}.

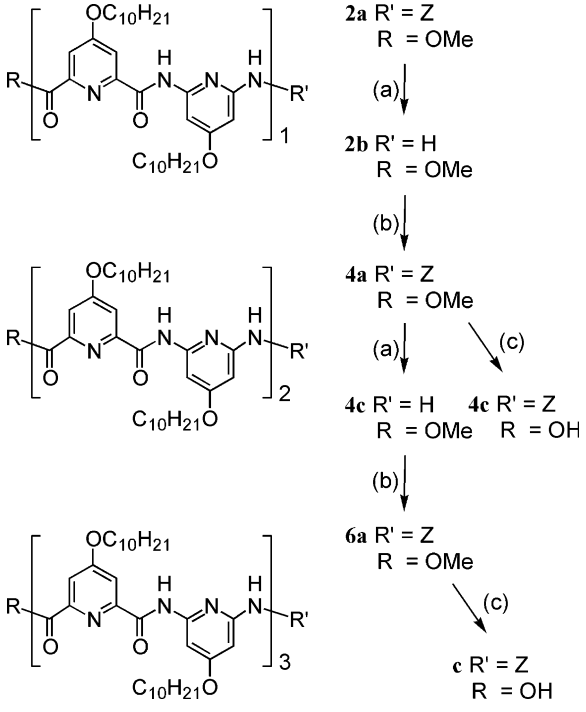

Scheme 2. Reagents and conditions: (a) DMF/MeOH, RT, H_2/Pd–C, quant. yield; (b) acid chloride of **2c**, toluene, iPr$_2$EtN, RT, 60–80% yield; (c) H_2O–dioxane, NaOH (2 equiv), RT, quant. Yield.

Dimerization constants at various temperatures were calculated by non linear regression analysis of the proportions of monomer and dimer measured from NMR signals at different concentrations. The values reported in Table 1 show that dimerization increases with strand length to reach a maximum value and that, somewhat counter-intuitively, it decreases for longer strands. At 25 °C, the value of K_{dim} increases with strand length from five to nine pyridine rings (up to 5200 L mol^{-1} for **9**), and decreases by 4 orders of magnitude for longer strands down to undetectable levels for **15**. This trend is even more pronounced at −19 °C where dimerization is strongly enhanced (Table 1): K_{dim} then reaches a maximum of 120,000 L mol^{-1} for compound **7**, and dramatically decreases for longer strands. The effect is still observed, though less intense, at 49 °C where dimerization is significantly lowered (Table 1).

These results are surprising because the number of stabilizing inter-strand interactions, and thus the stability of the double helices were expected to increase with increasing strand length. Indeed, oligomers often exhibit positive cooperativity upon hybridizing: not only the overall binding free energy ($-\Delta G^{\circ}$) increases with strand length,

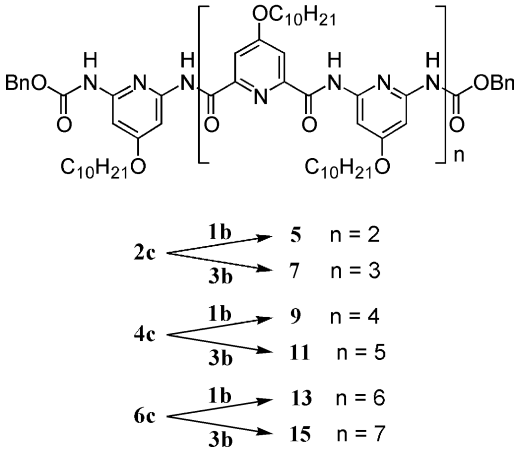

Scheme 3. Reagents and conditions: $SOCl_2$, reflux, then **1b** or **3b**, toluene, iPr$_2$EtN, RT, 20–40% yield.

Table 1. Values of K_{dim} (M^{-1})at various temperatures in $CDCl_3$

Entry	5	7	9	11	13	15
25 °C	210	1500	5200	650	65	—[a]
−19 °C	1900	120,000	42,800	920	180	—[a]
49 °C	—[b]	170	750	500	45	—[a]

[a] Signal intensity too low.
[b] Broad signals.

but also the binding free energy per monomer ($-\Delta G°/n$). For instance, this is the case in nucleic acids double helices and their analogs, and in several synthetic oligomers based on hydrogen bonding.[5,7,11]

To explain these results, we first hypothesized that the attractive interactions leading to duplex formation in oligopyridine dicarboxamides may not match over long strands. However, molecular models of long double helices built on the basis of the crystal structures of short double helices[19] show no alteration of the double helical motif (Fig. 3). Moreover even if the longer strands did not match over their entire length, they should still match along part of their length in the way short strands do and lead to some dimerization.

2.3. Stability of double helices and stability of single helices

The value of K_{dim} depends on the free energy difference between the double and the single helix. A drop in K_{dim} does not necessarily reflect a destabilization of the double helix. It may also result from a more important stabilization of the single helix. We thus sought for data indicating the effect of strand length on single helix stability on the one hand, and on double helix stability on the other hand.

Two independent indicators of single helix stability were followed by measuring ^{1}H NMR spectra of **5**–**15** at different temperatures: first, the extent of ring current effects on the protons belonging to the terminal units which can be deduced from the amplitude of the upfield shifts of their signals; and second the rate of inversion of the helix which is correlated to the temperature of coalescence of diastereopic patterns in the spectra.

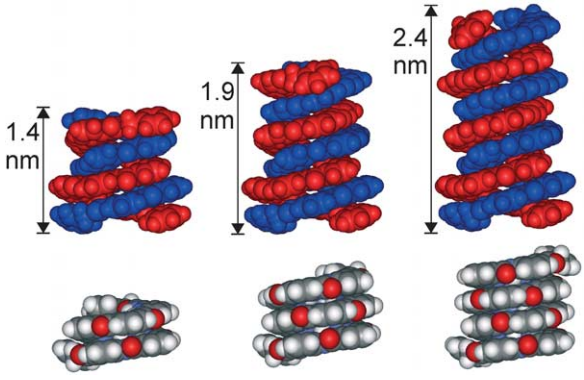

Figure 3. Molecular models of the double (top) and single (bottom) helices of compounds **7**, **11**, and **15**, obtained by prolongation of the patterns found in the crystal structures of previously described single and double helices,[18,19] followed by energy minimization (MM3). Alkoxy chains have been replaced by hydrogens for clarity.

In single helices, the environment of the protons belonging to the terminal units of the strand is not expected to depend much on the length of the strand beyond one helical turn. However, we observe that the signals of these protons undergo an upfield shift as strand length increases. For the signals of benzylic protons, the upfield shift is of almost 0.2 ppm between **7** and **15** (δ in Table 2). Similar shifts are observed for amide (Fig. 2) and aromatic (not shown) resonances. This reflects an increase of the ring current effects in the folded helical conformations and shows that short helices apparently spend more time in an extended form, whereas long helices apparently remain completely folded.

In the single helices, the terminal benzylic methylene protons give rise to two diastereotopic ^{1}H NMR signals which appear as doublets at ca. 4.8 and 5.2 ppm. Upon increasing temperature, these signals coalesce as the inversion of helix handedness becomes rapid on the NMR timescale (Fig. 4). The temperatures of coalescence recorded for **5**–**15** are reported in Table 2 (T_{inv}). The values of T_{inv} increase very rapidly with strand length: about +25° for every two pyridine rings added to the strand. For pentamer **5**, helix inversion becomes rapid on the NMR timescale above 10 °C. T_{inv} is found above the boiling point of $CDCl_3$ for nonamer **9** and undecamer **11** and even close to the boiling point of $C_2D_2Cl_4$ for the longest strands. Thus, these data give a qualitative but clear indication that the stability of the single helices with respect to unfolded states increases rapidly as oligomer length increases.

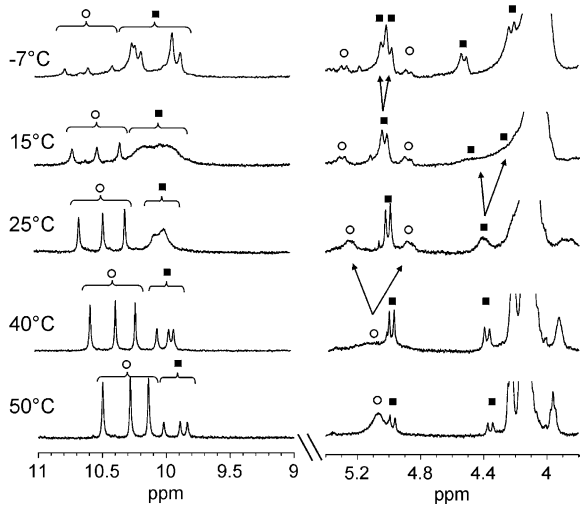

Figure 4. Part of the ^{1}H 400 MHz NMR spectra of compound **7**, C=1 mM in $CDCl_3$ at various temperatures, showing the resonances of the amides (11–9 ppm) and the resonnances of the benzylic methylenes (5.4–4.4 ppm). Some signals assigned to single helices and to the double helices are labelled by circles and squares respectively. Arrows indicate coalescences.

Table 2. Physical data for **5**–**15** in $CDCl_3$: chemical shift of one benzylic signal of the single helices (δ); temperatures of coalescence of 400 MHz ^1H NMR signals of diastereotopic protons of the single helice (T_{inv}) and of both ends of each strand in dissymmetrical degenerate double helices (T_{deg}); and estimated surfaces of the strands involved in π–π overlap in double helices (S_{dh} per strand) and single helices (S_{sh})

Compound	δ (ppm)	T_{inv}[a] (°C)	T_{deg}[b] (°C)	S_{dh} (Å^2)	S_{sh} (Å^2)	$\Delta = S_{dh} - S_{sh}$ (Å^2)
5	—[c]	10	36	500	200	300
7	4.86	43	3	760	450	310
9	4.78	65[d]	49	1020	710	310
11	4.75	90[d]	>55	1290	980	310
13	4.71	>120[d]	—[e]	1550	1230	320
15	4.69	>120[d]	—[e]	1820	1500	320

[a] Coalescence of benzylic protons at 5.2 and 4.8 ppm.
[b] Coalescence of benzylic protons at 4.95 and 4.93 ppm.
[c] Broad signal.
[d] In CD_2Cl_4.
[e] Signal intensity too low.

Two indicators of the stability of the double helices were also found. We initially expected to be able to measure the temperature of coalescence between the ^1H NMR signals of the single helix and the signals of the double helix. This temperature is close to room temperature for pentamer **5**, but it increases so rapidly with strand length that we could not access to this data for any other strand but heptamer **7** for which it was measured above 100 °C. The coalescence temperatures of longer strands are above the temperatures that one can reach with a standard NMR spectrometer. This result is corroborated by molecular dynamics simulations that we reported previously[19] that suggest that the rate of duplex dissociation is higher for shorter strands than for longer strands.

We also assessed the stability of the double helices by monitoring the sliding motion of the strands relative to one another within the duplex.[19] In double helices, the extremities of each strand are in a different environment, and the terminal benzylic methylene protons are not equivalent and give rise to two pairs of doublets between 5.2 and 4.4 ppm (Figs. 2 and 4). These four doublets are the signals of two pairs of diastereotopic protons which, in principle, can exchange upon inversion of the double helices. However, since the inversion of the double helix handedness requires dissociation of the strands, the coalescence between the diastereotopic signals of the double helix could not be observed in $CDCl_3$ (except for **5**, see above). Nevertheless, an equilibrium takes place between two degenerate states of the double helix allowing an exchange between the different environments of the strands.[19] When this equilibrium is fast on the NMR timescale, only two diastereotopic doublets are observed for the benzylic methylenes protons (Figs. 2 and 4). The temperatures of coalescence between the signals of these degenerate double helices (T_{deg} in Table 2) thus reflect the rate of an internal motion within the duplex. These temperatures also increase regularly with strand length from −36 °C for pentamer **5a** to over 55 °C for undecamer **11a**. For longer strands, T_{deg} could not be measured because the amount of double helix at high temperature is too low to be detected. This indicates slower dynamics in longer double helices, suggesting that the duplexes become more stable and that they do hybridize over their entire length.

In summary of this section, NMR data qualitatively show that, as could be expected, both double and single helices increase in stability as their length become longer. This arises from an increase of stabilizing interactions in both single and double helices, and results in a better helical organization and a decrease of the rates of dynamic motions as the length increases. However, these data alone give no hint why the variation of K_{dim} as a function of strand length goes through a maximum instead of following a monotonous increase or a monotonous decrease.

2.4. Enthalpic and entropic factors

Previous studies on the dimerization of oligopyridine dicarboxamides suggest that the main driving force of hybridization is interstrand π–π stacking.[19,20] The increase of stability of both single and double helices with increasing chain length presumably arises from an increase of intramolecular π–π overlap in the single helices (S_{sh} in Table 2) and of intermolecular π–π overlap in the double helices (S_{dh} in Table 2). In order to estimate S_{sh} and S_{dh}, we calculated the energy-minimized conformations of the single and double helices (Fig. 3), and compared the solvent accessible surfaces of these folded structures with those of linearly extended strands. As could be expected, the surface involved in π–π overlap increases linearly with strand length both in the single (S_{sh}) and in the double (S_{dh}) helices. However, the difference between S_{dh} and S_{sh} does not depend upon chain length and remains constant at ca. 300 Å^2, which is roughly the surface of the cross-section of one helix.[22] This result suggests that, in first approximation, the enthalpic gain of hybridization associated with π–π interactions is independent of strand length. One may argue that the nature of the stacked π-systems differ in the single and in the double helices,[23] and that the overall enthalpic gain may vary with strand length even though the surface involved in π-stacking does not increase. But the data show that this effect, if it exists, is not significant.

On the other hand, hybridization has an enthalpic cost associated with the extension of the strand and the doubling of the pitch (Fig. 1) that implies an increase of dihedral angles and a lengthening of the NH···N intramolecular hydrogen bonds within each strand of the duplex. This cost is directly proportional to the number of dihedral angles of the strand, and therefore increases linearly with strand length. The sum of an enthalpic cost that increases linearly with strand length and of an enthalpic gain that does not depend on strand length should lead to an overall decrease of the enthalpy of double helix formation as strand length increases.

We calculated the enthalpy of dimerization from van't Hoff plots for compounds **7**, **9** and **11**, for which K_{dim} can reliably be measured over a large temperature range. The results shown in Table 3 indeed show that the enthalpy of hybridization constantly decreases as the length of the oligomer increases. The enthaplic term is very strong for heptamer **7** ($\Delta H = -64 \pm 3$ kJ mol^{-1}) as the increase of the surface involved in π–π overlap from single to double helix is large relative to the overall surface of the strand. For nonamer **9**, the enthalpic gain of dimerization is smaller ($\Delta H = -42 \pm 4$ kJ mol^{-1}). For compound **11**, the enthalpic term reaches very low levels ($\Delta H = -5.8 \pm 0.4$ kJ mol^{-1}) which reflects the fact the gain in π–π overlap upon dimerization is largely compensated by the cost of helix extension.

From these results, it seems reasonable to propose that the drop of K_{dim} for longer oligomers results from a drop of the enthalpic gain of hybridization. It remains to explain why K_{dim} goes through a maximum and does not follow a monotonous decrease. The van't Hoff plots for compounds **7**, **9** and **11** show that the entropy of hybridization follows a trend opposite to that of the enthalpy. The large ΔH for **7** is compensated by a large negative entropic term ($\Delta S = -154 \pm 9$ J K^{-1} mol^{-1}). The entropic loss during hybridization is smaller for **9** ($\Delta S = -74 \pm 14$ J K^{-1} mol^{-1}), and even has a (small) positive value ($\Delta S = 34 \pm 1$ J K^{-1} mol^{-1}) for **11**. This trend of the entropy of hybridization as a function of length presumably reflects that the helical preorganization of the monomers increases with strand length, which allows the longer strands to hybridize with a minimal loss of motional freedom, that is to say at a low entropic price. The positive value of ΔS for **11** suggests that other factors are at play, possibly desolvation, which may contribute favorably to dimerization.

It is worth noting that the large value of ΔS for **7** results in a strong temperature dependence of K_{dim}: by up to three orders of magnitude over a range of 75° (Table 3 and Fig. 4). On the other hand, dimerization of the longer strands show very little temperature dependence (Table 3): only a factor of 2 over a range of 75°.

The hybridization behavior of AOA's contrasts with that of most artificial and natural oligomers. The major difference is that not only the dimers of AOA's fold into well organized structures, but also the monomers. For instance, single stranded DNA, does not generally adopt a stable and well-defined conformation. However, when this is possible as, for example, in hairpins or in G-quartets, hybridization into double helices is impeded.[24] A few artificial oligomers capable of pairing into duplexes reported in the literature also form stable single stranded structures, and it will be interesting to see whether these oligomers keep their ability to hybridize as the strands get longer.

3. Conclusion

In summary, we have presented a new synthetic scheme for the preparation of AOA's and studied their hybridization into double helices as a function of strand length. The fact that the enthalpic price of spring-like extension that a strand must undergo during the formation of a double helix is not compensated by intermolecular π–π interactions explains that dimerization of AOA's decreases for longer oligomers. That K_{dim} goes through a maximum before decreasing results from entropic effects that partially compensate for the decreasing enthalpy of hybridization. These results suggest that a subtle destabilization of the single helical monomers might enhance their hybridization into double helices. Studies on these effects and also on the role of the side chains, and of terminal residues, are currently underway and will be reported in due course.

4. Experimental

4.1. General

Solvents (THF, toluene, CH_2Cl_2) were dried by filtration over activated alumina on a commercially available setup. FTIR spectra were recorded on a Brucker IFS 55 FT-IR Spectrometer 400 MHz ^{1}H and 100 MHz ^{13}C NMR spectra were recorded on a Bruker 400 Ultrashield spectrometer. The chemical shifts are expressed in parts per million (ppm) using the residual solvent peak as an internal standard. The following notations are used for the ^{1}H NMR spectral splitting patterns: singlet (s), doublet (d), triplet (t), multiplet (m), borad (br). Melting points are uncorrected. Diester **1a** and diamine **1b** were prepared as described previously.

4.1.1. 4-Decyloxy-2,6-pyridinedicarboxylic acid monomethyl ester (1c). Dimethyl 4-decyloxy-2,6-pyridinedicarboxylate[19] (2.1 g, 6 mmol) was dissolved in 1,4-dioxane (32 mL) and methanol (8 mL) and the solution was cooled to 0 °C. Sodium hydroxide (0.24 g, 6 mmol) was added and the mixture was stirred at 0 °C for 2 h and another 2 h at ambient temperature. The solution was neutralized with acetic acid and poured into water (100 mL). The product was extracted with CH_2Cl_2 (2×50 mL). The organic phase was evaporated and dried under vacuum. The product contaminated with small amounts of starting diester was used without further purification. Yield 1.7 g (85%) of a white solid. Mp: 91–92 °C. ^{1}H NMR ($CDCl_3$), δ 7.84 (1H, s), 7,80 (1H, s), 4.15 (2H, t, J=6.7 Hz), 4.01 (3H, s), 1.84 (2H, m), 1.47 (2H, m), 1,27 (15H, m). TOF-MS (*m/z*): 338.37 $[M+H]^+$ (Calcd for $C_{18}H_{28}NO_5$: 338.20).

4.1.2. (6-Amino-4-decyloxy-pyridin-2-yl)-carbamic acid benzyl ester (1d). To a solution of 4-decyloxy-2,6-diaminopyridine **1b**[19] (1.5 g, 5.65 mmol) in anhydrous

Table 3. Values of K_{dim} (M^{-1}) at various temperatures for and values of ΔH and ΔS **7**, **9** and **11**

Compound	T (°C)							ΔH (kJ mol^{-1})	ΔS (J K^{-1} mol^{-1})
	−19	−4	10	25	36	−49	55		
7	120,000	22,000	12,000	1500	710	170	140	−64±3	−154±9
9	42,800	23,200	10,300	5200	2500	750	400	−42±4	−74±14
11	920	750	710	650	560	500	480	−5.8±0.4	34±1

THF at −78 °C (60 mL) was slowly added a 2 M solution of *n*-butyllithium in hexane (2.7 mL, 1 equiv) After 15 min, benzyl chloroformate (934 μL, 1 equiv) was added at once. The mixture was stirred at −78 °C for 5 h, then at room temperature for 12 h. The reaction was quenched with a small amount of water. The solvent was evaporated, and the residue was dissolved in CH_2Cl_2. This solution was washed with water, dried ($MgSO_4$), filtered and evaporated. The residue was purified by flash chromatography on silica gel eluting with CH_2Cl_2/AcOEt. Yield 1.5 g (67%) of an off-white solid. Mp: 85–87 °C. ^{1}H NMR ($CDCl_3$) δ 7.56 (1H, s), 7.36 (5H, m), 6.97 (1H, s), 5.69(1H, s), 5.87 (2H, s), 4.21 (2H, s), 3.95 (2H, t, J=6.8 Hz), 1.74 (2H, m), 1.27 (14H, m), 0.89 (3H, t, J=6.8 Hz). ^{13}C NMR ($CDCl_3$) δ 168.65, 158.51, 153.08, 151.57, 135.86, 128.51, 128.25, 128.16, 89.86, 89.22, 67.89, 66.85, 31.85, 29.50, 29.27, 28.94, 25.88, 22.64, 14.08. IR (liquid layer) ν (cm^{-1}): 3450, 3343, 3258, 3208, 3201, 2957, 2942, 2920, 2873, 2852, 1743, 1718, 1658, 1611, 1578, 1562, 1468, 1454, 1444, 1440, 1405, 1332, 1321, 1313, 1291, 1241, 1226, 1190, 810, 753, 731. TOF-MS (*m*/*z*): 400.35 $[M+H]^+$ (Calcd for $C_{23}H_{34}N_3O_3$: 400.26).

4.1.3. Trimeric diamine 3b. To a solution of 4-decyloxy-2,6-diaminopyridine (0.5 g, 1.88 mmol) in anhydrous THF (4 mL) at −78 °C, was added *n*-butyllithium (2.1 M, 0.942 mL, 1.05 equiv). The mixture was allowed to stand at −78 °C for 15 min. A solution of dimethyl 4-decyloxy-2,6-pyridinedicarboxylate (0.278 g, 0.79 mmol, 0.42 equiv) in THF (3 mL) was added using a canula. The mixture was stirred at −78 °C for 4 h, then at ambient temperature for 24 h. The reaction was quenched with acetic acid (1.2 equiv) and then evaporated to dryness. The residue was purified by flash chromatography on silica gel eluting with ethyl acetate/cyclohexane 2:1 vol/vol, to afford **3b**. Yield 259 mg (40% from the diester) of a yellow wax. ^{1}H NMR ($CDCl_3$, ppm) δ 9.99 (2H, s), 7.86 (2H, s), 7.35 (2H, s), 5.66 (2H, s), 5.27 (4H, br), 4.10 (2H, t, J=6,7 Hz), 3.86 (4H, t, J=6.7 Hz), 1.70 (6H, m), 1.28 (42H, m), 0.89 (9H, m). ^{13}C NMR ($CDCl_3$): 168.72, 168.15, 161.38, 158.42, 150.27, 111.52, 91.58, 90.12, 69.16, 68.07, 52.74, 31.87, 29.67, 29.56, 29.38, 29.27, 29.00, 25.91, 25.80, 22.65, 14.08. IR (liquid layer) ν (cm^{-1}): 3361, 2924, 2854, 1694, 1613, 1578, 1535, 1448, 1378, 1344, 1175, 1048.

4.2. Synthesis of 2a, 4a and 6a. General method for coupling a monoacid and a monoamine

Under an anhydrous atmosphere, a solution of acid **1c** or **2c** (1 mmol) in thionyl chloride (5 mL) was heated to reflux till evolvement of gas stopped (ca 30–60 min). The excess thionyl chloride was distilled under reduced pressure, and azeotroped with dry toluene. The residue was dissolved in dry toluene (10 mL). To this solution at 0 °C was added a solution of amine **1d**, **2b** or **4b** (0.9 equiv) in dry toluene (10 mL), followed by distilled *N*,*N*-diisopropylethylamine (5 equiv). The mixture was allowed to warm to ambient temperature and stirred overnight. The solvent was removed and the residue was purified by flash chromatography on silica gel.

4.2.1. Dimer 2a. From acid **1c** (2.026 g, 6.0 mmol) and amine **1d** (2 g, 5.0 mmol). The residue was purified by flash chromatography on silica gel eluting with cyclohexane/EtOAc 10:1 vol/vol. Yield 2.63 g (73%) of a white solid. Mp: 107–109 °C ^{1}H NMR ($CDCl_3$), δ 10.19 (1H, s), 7.91 (1H, d, J=2.8 Hz), 7.75 (1H, d, J=2 Hz), 7.68 (1H, d, J=2 Hz), 7.32 (6H, m), 5.22 (2H, s), 4.15 (2H, t, J=6 Hz), 4.07 (2H, t, J=6.8 Hz), 4.02 (3H, s), 1.82 (4H, m), 1.28 (28H, m), 0.88 (6H, t, J=6.8 Hz). ^{13}C NMR ($CDCl_3$): δ 169.00, 167.64, 165.01, 161.74, 152.84, 151.27, 150.99, 150.19, 148.45, 135.78, 128.58, 128.11, 111.01, 95.88, 94.84, 69.14, 68.43, 67.08, 52.97, 31.85, 29.48, 29.30, 29, 28.94, 28.68, 25.89, 25.80, 22.65, 14.09. IR (KBr) ν (cm^{-1}) 3363, 2919, 2852, 1732, 1713, 1695, 1602, 1580, 1537, 1509, 1444, 1354, 1332, 1262, 1215, 1172, 1151, 1092, 1042. TOF-MS (*m*/*z*): TOF-MS 719.46 $[M+H]^+$ (Calcd for $C_{41}H_{59}N_4O_7$: 719.44), 741.45 $[M+Na]^+$, 757.42 $[M+K]^+$.

4.2.2. Tetramer 4a. From acid **2c** (1.44 g, 2.0 mmol) and amine **2b** (1.0 g, 1.7 mmol). The residue was purified by flash chromatography on silica gel eluting with cyclohexane/EtOAc 10:1 vol/vol. Yield 1.78 g (82%) of a white wax. ^{1}H NMR ($CDCl_3$) δ 10.60 (1H, s), 10.52 (1H, s), 10.50 (1H, s), 8.42 (1H, br), 7.83 (1H, d, J=2 Hz), 7.77 (1H, d, J=2 Hz), 7.75 (1H, d, J=2 Hz), 7.64 (1H, s), 7.57 (2H, m), 7.40 (1H, d, J=2 Hz), 7.11 (5H, m), 7.01 (1H, d, J=3 Hz), 4.85 (2H, s), 4.15 (2H, t, J=6.8 Hz), 4.04 (4H, t, J=6 Hz), 3.97 (2H, t, J=6.4 Hz), 3.67 (3H, s), 1.82 (8H, m), 1.30 (56H, m), 0.89 (12H, t, J=6.8 Hz). ^{13}C NMR ($CDCl_3$) δ 168.92, 168.14, 167.40, 164.61, 161.74, 161.56, 152.91, 151.30, 150.56, 150.47, 150.27, 147.52, 135.51, 128.22, 127.83, 127.35, 114.75, 111.60, 110.90, 97.21, 96.77, 96.05, 95.16, 69.22, 69.08, 68.54, 68.42, 66.62, 52.83, 31.90, 29.58, 29.55, 29.31, 29.00, 28.78, 25.94, 25.84, 22.68, 14.11. IR (KBr) ν (cm^{-1}): 2924, 2854, 1736, 1699, 1580, 1522, 1438, 1338, 1218, 1173, 1108, 1088, 1046, 1018. TOF-MS (*m*/*z*): 1271.76 $[M+H]^+$ (Calcd for $C_{73}H_{107}N_8O_{11}$: 1271.81).

4.2.3. Hexamer 6a. From acid **2c** (0.26 g, 0.37 mmol) and amine **4b** (0.35 g, 0.31 mmol). The residue was purified by flash chromatography on silica gel eluting with toluene/EtOAc 95:5 vol/vol. Yield 390 mg (69%) of a white wax. ^{1}H NMR ($CDCl_3$, 36 °C, 1 mM) δ 10.86 (1H, s), 10.70 (1H, s), 10.46 (1H, s), 10.26 (1H, s), 10.08 (1H, s), 7.94 (1H, br), 7.89 (1H, br), 7.78 (1H, br), 7.80 (1H, br), 7.72 (2H, br), 7.52 (1H, br), 7.43 (1H, br), 7.34 (3H, br), 7.14 (5H, br), 7.00 (2H, br), 5.10 (2H, s), 4.16 (24H, m), 3.64 (3H, s), 1.88 (6H, br), 1.33 (84H, m), 0.91 (12H, s). ^{13}C NMR ($CDCl_3$) δ 168.80, 168.00, 167.78, 167.43, 166.95, 164.5, 164.30, 161.39, 160.62, 151.28, 150.27, 150.18, 149.86, 149.44, 135,51, 134.97, 128.83, 128.15, 127.65, 127.18, 114.88, 114.20, 11.49, 111.22, 111.00, 110.36, 110.11, 97.39, 96.64, 96.56, 95.09, 94.70, 69.10, 68.63, 68.01, 66.10, 52.86, 52.48, 31.95, 29.68, 29.42, 29.06, 25.93, 22.71, 14.13. IR (KBr) ν (cm^{-1}): 3372, 2924, 2854, 1735, 1696, 1583, 1523, 1438, 1339, 1218, 1174, 1121, 1046, 849. TOF-MS (*m*/*z*): 1824.06 $[M+H]^+$ (Calcd for $C_{105}H_{155}N_{12}O_{15}$: 1824.17).

4.3. Synthesis of 2b and 4b. General hydrogenation procedure

A mixture of benzylcarbamate **2a** or **4a** (1 mmol) dissolved in DMF (10 mL) and methyl alcohol (10 mL), and of 10% Pd/C (10% weigh) was stirred overnight under hydrogen at

atmospheric pressure The mixture was filtered through Celite. The solvents were removed under reduced pressure to give the product, which was used without further purification.

4.3.1. Synthesis of dimer amine 2b. From dimer **2a** (1 g, 1.39 mmol) and 10% Pd/C (100 mg). Yield 810 mg (quantitative) of **2b** as an off-white solid. Mp: 160–161 °C. ^{1}H NMR ($CDCl_3$) δ 10.15 (1H, s), 7.92 (1H, d, J=2.8 Hz), 7.74 (1H, d, J=2 Hz), 7.46 (1H,d, J=2 Hz), 5.83 (1H, d, J=2 Hz), 4.32 (2H, s), 4.14 (2H,t, J=6.8 Hz), 4.02 (5H, m), 1.82 (4H, m), 1.28 (28H, m), 0.88 (6H, t, J=6.8 Hz). ^{13}C NMR ($CDCl_3$) δ 168.61, 167.61, 165.01, 158.84, 151.61, 150.62, 148.10, 114.91, 110.82, 91.36, 90.32, 69.10, 68.00, 52.90, 31.85, 29.54, 29.49, 29.28, 29.02, 28.70, 25.93, 25.80, 22.64, 14.09. IR (KBr) ν (cm^{-1}): 3404, 3343, 2920, 2851, 1723, 1702, 1658, 1614, 1597, 1532, 1464, 1382, 1347, 1294, 1254, 1165, 1107, 1040. TOF-MS (*m*/*z*): 585.49 $[M+H]^+$ (Calcd for $C_{33}H_{53}N_4O_5$: 585.40).

4.3.2. Synthesis of tetramer amine 4b. From tetramer **4a** (0.95 g) and 10% Pd/C (80 mg). Yield 850 mg (quantitative) of **4b** as an off-white wax. ^{1}H NMR ($CDCl_3$) δ 10.61 (1H, s), 10.47(1H, s), 10.39 (1H, s), 7.91 (4H, m), 7.73 (1H, s), 7.70 (1H, s), 7.51(1H, s), 5.81 (1H, s), 4.16 (6H, m), 4.01(2H, t, J=6 Hz), 3.95 (2H, s), 3.50 (3H, s), 1.84 (8H, m), 1.29 (56H, m), 0.89 (12H, t, J=7.4 Hz). TOF-MS (*m*/*z*): 1137.87 (Calcd for $C_{65}H_{101}N_8O_9$: 1137.77).

4.4. General method for the saponification of methyl esters

To a solution of ester **2a**, **4a**, or **6a** (1.39 mmol) in 1,4-dioxane (20 mL) and water (2 mL), was added sodium hydroxide (111.2 mg; 2 equiv). The resulting solution was stirred for 2 h at 25 °C, and then neutralized with an excess of AcOH. The solution was extracted with dichloromethane (40 mL). The organic phase was washed with water, dried over $MgSO_4$, filtered and evaporated, to yield the corresponding acid which was used without further purification. Following this procedure, dimer acid **2c**, tetramer acid **4c** and hexamer acid **6c** were obtained as off-white solids in quantitative yield. Dimer **2c** could be characterized by ^{1}H NMR but **4c** and **6c** show very broad spectra due to the single helix-double helix equilibrium and non-specific aggregation involving the carboxylic acid group. Complete conversion was confirmed by thin layer chromatography and the absence of methyl ester signal on the NMR spectra.

4.4.1. Dimer 2c. Mp: 176–177 °C. ^{1}H NMR ($CDCl_3$) δ 10.76 (1H, s), 8.03 (1H, s), 7.96 (1H, d, J=2.7 Hz), 7.90 (1H, d, J=2.7 Hz), 7.78 (1H, d, J=2 Hz), 7.41 (6H, m), 5.25 (2H, s), 4.16 (2H, dd, J_1=6.7 Hz, J_2=6 Hz), 4.09 (2H, dd, J_1=6.7 Hz, J_2=6 Hz), 1.83 (4H, m), 1.46 (4H, m), 1.28 (24H, s), 0.88 (6H, m). HR TOF-MS (*m*/*z*): 705.54 $[M+H]^+$ (Calcd for $C_{40}H_{57}N_4O_7$: 705.42).

4.5. Synthesis of oligomers 5, 7, 9, 11, 13 and 15. General method coupling an acid and a diamine

The procedure is the same as for coupling a monoacid and a monoamine (see Section 4.2), except that only 0.4 equiv of diamine were used. All products were purified by flash chromatography on silica gel eluting with cyclohexane/EtOAc 95/5 vol:vol.

4.5.1. Pentamer 5. From diameric acid **2c** (300 mg, 0.42 mmol)) and monomeric diamine **1b** (47 mg, 0.18 mmol). Yield 69 mg (25%) of a white wax. ^{1}H NMR ($CDCl_3$, 36 °C, 1 mM, signals of the single helix) δ 10.35 (4H, br), 7.85 (4H, br), 7.03 (2H, br, m), 7.15 (10H, br, m), 7.03 (6H, br, m), 5.03 (4H, br, m), 4.08 (10H, br, m), 1.86 (10H, br, m), 1.31 (70H, br, m), 0.91 (15H, br, m). IR (KBr) ν (cm^{-1}): 2924, 2854, 1697, 1586, 1533, 1453, 1339, 1217, 1175, 1045. HR TOF-MS (*m*/*z*): 1639.04 $[M+H]^+$ (Calcd for $C_{95}H_{136}N_{11}O_{13}$: 1639.03).

4.5.2. Heptamer 7. From dimeric acid **2c** (72 mg, 0.1 mmol) and trimeric diamine **3b** (36.5 mg, 0.045 mmol). Yield 34.21 mg (35%) of a white wax. ^{1}H NMR ($CDCl_3$, 36 °C, 1 mM, signals of the single helix) δ 10.60 (2H, s), 10.41 (2H, s), 10.25 (2H, s), 7.88 (2H, s), 7.79 (2H, s), 7.65 (2H, s), 7.49 (2H, s), 7.32 (2H, s), 7.13 (7H, m), 7.03 (7H, m), 7.00 (2H, s), 5.23 (2H, br), 4.89 (2H, br), 4.22 (2H, br), 4.14 (12H, br), 1.88 (14H, br), 1.34 (98H, br, m), 0.91 (21H, br, m). ^{13}C NMR ($CDCl_3$) δ 169.25, 168.92, 168.11, 167.91, 167.41, 167.31, 163.82, 161.41, 161.05, 160.92, 151.66, 150.22, 150.06, 149.77, 149.46, 148.79, 135.44, 130.86, 128.78, 128.21, 127.74, 127.17, 126.77, 111.65, 111.41, 111.26, 110.93, 96.96, 96.75, 96.28, 95.63, 94.06, 69.22, 68.07, 66.31, 37.39, 33.68, 32.75, 31.93, 30.17, 29.68, 29.40, 29.05, 27.30, 26.05, 25.93, 22.71, 19.73, 14.13. IR (liquid layer) ν (cm^{-1}): 3313, 2957, 2924, 2853, 1735, 1700, 1648, 1616, 1585, 1579, 1560, 1540, 1523, 1458, 1430, 1377, 1349, 1339, 1261, 1218, 1176, 1092, 1052, 1020. TOF-MS (*m*/*z*): 2191.27 $[M+H]^+$ (Calcd for $C_{127}H_{184}N_{15}O_{17}$: 2191.40).

4.5.3. Nonamer 9. From tetrameric acid **4c** (103 mg, 0.082 mmol) and monomeric diamine **1b** (8.68 mg, 0.033 mmol). Yield 19.2 mg (21%) of a white wax. ^{1}H NMR ($CDCl_3$, 36 °C, 1 mM, signals of the single helix) δ 10.65 (2H, s), 10.40 (2H, s), 10.34 (2H, s), 10.32 (2H, s), 7.90 (2H, d, J=2 Hz), 7.62 (4H, d, J=2 Hz), 7.59 (4H, d, J=2 Hz), 7.54 (2H, d, J=2 Hz), 7.58 (2H, s), 7.44 (2H, d, J=2 Hz), 7.18 (2H, d, J=2 Hz), 7.10 (10H, br), 6.87 (2H, d, J=2 Hz), 5.18 (2H, d, J=12.8 Hz), 4.79 (2H, d, J=12.8 Hz), 4.10 (18H, br, m), 1.93 (18H, br, m), 1.33 (126H, br, m), 0.91 (27H, br, m). ^{13}C NMR ($CDCl_3$) δ 168.08, 167.91, 167.72, 167.17, 161.18, 160.77, 160.70, 151.55, 150.17, 149.85, 149.67, 149.36, 128.16, 127.71, 127.17, 111.30, 111.11, 95.95, 95.60, 94.20, 69.17, 68.03, 31.92, 29.73, 29.68, 29.35, 29.06, 28.87, 26.11, 25.97, 22.68, 14.13. IR (liquid layer) ν (cm^{-1}): 2956, 2923, 2853, 1740, 1699, 1613, 1585, 1523, 1439, 1389, 1261, 1217, 1176, 1092, 1046. HR TOF-MS (*m*/*z*): 2744.03 $[M+H]^+$ (Calcd for $C_{160}H_{233}N_{18}O_{21}$: 2742.77).

4.5.4. Undecamer 11. From tetrameric acid **4c** (55 mg, 0.044 mmol) and trimeric diamine **3b** (17 mg, 0.021 mmol). Yield 23.4 mg (34%) of a white wax. ^{1}H NMR ($CDCl_3$, 36 °C, 1 mM, single helix, ppm) δ 10.45 (4H, s), 10.40 (2H, s), 10.20 (2H, s), 10.07 (2H, s), 7.80 (2H, d, J=2 Hz), 7.63 (2H, d, J=2 Hz), 7.57 (2H, s), 7.55 (2H, d, J=2 Hz), 7.45 (2H, d, J=2 Hz), 7.33 (2H, d, J=2 Hz), 7.28 (5H, br), 7.20

(5H, br), 7.14 (2H, d, $J=2$ Hz), 7.04 (2H, s), 7.02 (2H, s), 6.95 (2H, s), 6.93(2H, s), 6.81 (2H, s), 5.17 (2H, d, $J=$ 12 Hz), 4.76 (2H, d, $J=12.8$ Hz), 4.12 (22H, br, m), 1.91 (22H, br, m), 1.34 (154H, br, m), 0.93 (33H, br, m). ^{13}C NMR ($CDCl_3$) δ 168.03, 167.85, 167.64, 167.55, 167.13, 167.04, 161.24, 161.06, 160.61, 160.52, 151.05, 150.14, 149.94, 149.56, 149.34, 149.24, 149.12, 148.82, 148.61, 135.51, 135.33, 130.92, 128.83, 128.15, 127.70, 127.17, 111.65, 111.46, 111.13, 110.82, 95.93, 95.76, 95.51, 69.11, 67.88, 66.52, 66.05, 32.08, 31.90, 30.12, 29.65, 29.40, 29.33, 29.05, 25.99, 25.80, 22.80, 22.711, 14.14. IR (liquid layer) ν (cm^{-1}): 2924, 2854, 1702, 1611, 1581, 1517, 1438, 1339, 1216, 1175, 1048. TOF-MS (*m/z*): 3113.38 $[M+H-2(C_7H_8)]^+$, 3136.24 $[M+Na-2(C_7H_8)]^+$, 3152.24 $[M+K-2(C_7H_8)]^+$ (Calcd for $C_{177}H_{266}N_{23}O_{25}$: 3114.03).

4.5.5. Tridecamer 13. From hexameric acid **6c** (128 mg) and monomeric diamine **1b** (7.0 mg). Yield 31.5 mg (31%) of a white wax. ^{1}H NMR ($CDCl_3$, 25 °C, 1 mM, signals of the single helix) δ 10.29 (2H, s), 10.28 (2H, s), 10.25 (2H, s), 10.18 (2H, s), 10.14 (2H, s), 10.10 (2H, s), 7.79 (2H, s), 7.47 (2H, s), 7.39 (2H, s), 7.37 (2H, s), 7.17 (10H, br, m), 7.02 (4H, s), 6.98 (4H, br, m), 6.96 (2H, s), 6.88 (2H, s), 6.86 (2H, s), 6.84 (2H, s), 6.77 (2H, s), 5.13 (2H, d, $J=12.8$ Hz), 4.72 (2H, d, $J=12.8$ Hz), 4.08 (26H, br, m), 1.96 (26H, br, m), 1.35 (182H, br, m), 0.92 (33H, br, m). ^{13}C NMR ($CDCl_3$) δ 168.86, 168.56, 168.02, 167.62, 167.23, 166.99, 166.90, 161.21, 160.83, 160.62, 160.41, 159.26, 153.74, 151.54, 150.09, 149.86, 149.77, 149.53, 149.40, 149.17, 149.00, 148.66, 148.55, 148.34, 135.68, 135.32, 128.10, 127.91, 127.65, 127.17, 126.53, 111.58, 111.38, 111.11, 110.96, 110.86, 96.55, 95.88, 95.70, 95.568, 95.46, 69.07, 68.50, 67.94, 67.82, 66.46, 31.95, 30.15, 29.82, 29.67, 29.56, 29.41, 29.11, 26.05, 22.73, 14.14. IR (liquid layer) ν (cm^{-1}): 2924, 2854, 1700, 1615, 1585, 1524, 1439, 1389, 1339, 1216, 1175, 1046. TOF-MS (*m/z*): 3666.66 $[M+H-2(C_7H_8)]^+$, 3688.45 $[M+Na-2(C_7H_8)]^+$ (Calcd for $C_{209}H_{314}N_{27}O_{29}$: 3666.39).

4.5.6. Pentadecamer 15. From hexameric acid **6c** (90 mg) and trimeric diamine **3b** (16.3 mg). Yield 1.9 mg (2.2%) as a white wax. ^{1}H NMR ($CDCl_3$, 25 °C, 1 mM, signals of the single helix) δ 10.32 (2H, s), 10.29 (2H, s), 10.25 (2H, s), 10.20 (2H, s), 10.11 (2H, s), 9.98 (2H, s), 9.96 (2H, s), 7.76 (2H, s), 7.46 (2H, s), 7.36 (2H, s), 7.34 (2H, s), 7.20 (5H, s), 7.17 (2H, s), 7.13 (2H, s), 7.08 (5H, s), 7.06 (2H, s), 7.02 (2H, s), 7.00 (2H, s), 6.98 (2H, s), 6.95 (2H, s), 6.88 (4H, br), 6.85 (2H, s), 6.79 (2H, s), 6.75 (2H, s), 5.12 (2H, d, $J=$ 12.8 Hz), 4.71 (2H, d, $J=12.8$ Hz), 4.06 (30H, br, m), 1.86 (30H, br, m), 1.35 (210H, br, m), 0.92 (45H, br, m), IR (liquid layer) ν (cm^{-1}): 2923, 2853, 1701, 1585, 1524, 1439, 1340, 1045. TOF-MS (*m/z*): 4228.65 $[M+H-2(C_7H_8)]^+$, 4240.07 $[M+Na-2(C_7H_8)]^+$, 4256.03 $[M+K-2(C_7H_8)]^+$ (Calcd for $C_{241}H_{362}N_{31}O_{33}$: 4218.76).

Acknowledgements

This work was supported by the Centre National de la Recherche Scientifique, the Région Aquitaine (predoctoral fellowship to V. M.), the University of Bordeaux I and by the Ministère de la Recherche (postdoctoral fellowship to H. J.).

References and notes

1. Hill, D. J.; Mio, M. J.; Prince, R. B.; Hughes, T. S.; Moore, J. S. *Chem. Rev.* **2001**, *101*, 3893–4011.
2. Nielsen, P. E. *Acc. Chem. Res.* **1999**, *32*, 624–630.
3. Sessler, J. L.; Wang, R. *J. Am. Chem. Soc.* **1996**, *118*, 9808–9809. Sessler, J. L.; Wang, R. *Angew. Chem., Int. Ed.* **1998**, *37*, 1726–1729.
4. Di Blasio, B.; Benedetti, E.; Pavone, V.; Pedone, C. *Biopolymers* **1989**, *28*, 203–214. Langs, D. A. *Science* **1988**, *241*, 188–191. Burkhart, B. M.; Gassman, R. M.; Langs, D. A.; Pangborn, W. A.; Duax, W. L.; Pletnev, V. *Biopolymers* **1999**, *51*, 129–144.
5. Gong, B.; Yan, Y.; Zeng, H.; Skrzypczak-Jankunn, E.; Wah Kim, Y.; Zhu, J.; Ickes, H. *J. Am. Chem. Soc.* **1999**, *121*, 5607–5608. Zeng, H.; Miller, R. S.; Flowers, R. A.; Gong, B. *J. Am. Chem. Soc.* **2000**, *122*, 2635–2644. Zeng, H.; Ickes, H.; Flowers, R. A.; Gong, B. *J. Org. Chem.* **2001**, *66*, 3574–3583. Zeng, H.; Yang, X.; Flowers, R. A.; Gong, B. *J. Am. Chem. Soc.* **2002**, *124*, 2903–2910. Yang, X.; Martinovic, S.; Smith, R. D.; Gong, B. *J. Am. Chem. Soc.* **2003**, *125*, 9932–9933.
6. Corbin, P. S.; Zimmerman, S. C. *J. Am. Chem. Soc.* **2000**, *122*, 3779–3780. Corbin, P. S.; Zimmerman, S. C.; Thiessen, P. A.; Hawryluk, N. A.; Murray, T. J. *J. Am. Chem. Soc.* **2001**, *123*, 10475–10488.
7. Archer, E. A.; Goldberg, N. T.; Linch, V.; Krische, M. J. *J. Am. Chem. Soc.* **2000**, *122*, 5006–5007. Archer, E. A.; Cauble, D. F.; Lynch, V.; Krische, M. J. *Tetrahedron* **2001**, *58*, 721–725. Archer, E. A.; Krische, M. J. *J. Am. Chem. Soc.* **2002**, *124*, 5074–5083.
8. Schmuk, C.; Lex, J. *Eur. J. Org. Chem.* **2001**, 1519–1523. Schmuck, C.; Wienand, W. *J. Am. Chem. Soc.* **2003**, *125*, 452–459.
9. Moriuchi, T.; Tamura, T.; Hirao, T. *J. Am. Chem. Soc.* **2002**, *124*, 9356–9357.
10. Folmer, B. J. B.; Sijbesma, R. P.; Kooijman, H.; Spek, A. L.; Meijer, A. W. *J. Am. Chem. Soc.* **1999**, *121*, 9001–9007.
11. Bisson, A. P.; Carver, F. J.; Eggleston, D. S.; Haltiwanger, R. C.; Hunter, C. A.; Linvingstone, D. L.; MacCabe, J. F.; Rotger, C.; Rowan, A. E. *J. Am. Chem. Soc.* **2000**, *122*, 8856–8868.
12. Nowick, J. S.; Chung, D. M.; Maitra, K.; Maitra, S.; Stigers, K. D.; Sun, Y. *J. Am. Chem. Soc.* **2000**, *122*, 7654–7661.
13. For reviews on helicates: Albrecht, M. *Chem. Rev.* **2001**, *101*, 3457–3498. Piguet, C.; Bernardinelli, G.; Hopfgartner, G. *Chem. Rev.* **1997**, *97*, 2005–2062.
14. Sànchez-Quesada, J.; Seel, C.; Prados, P.; de Mendoza, J. *J. Am. Chem. Soc.* **1996**, *118*, 277–278. Keegan, J.; Kruger, P. E.; Nieuwenhuyzen, N.; O'Brien, J.; Martin, N. *Chem. Commun.* **2001**, 2192–2193. Coles, S. J.; Frey, J. G.; Gale, P. A.; Hursthouse, M. B.; Light, M. E.; Navakun, K.; Thomas, G. L. *Chem. Commun.* **2003**, 563–564.
15. Gabriel, G. J.; Iverson, B. L. *J. Am. Chem. Soc.* **2002**, *124*, 15174–15175.
16. For a review see: Huc, I. *Eur. J. Org. Chem.* **2004**, 17–29.
17. For recent examples: Odriozola, I.; Kyritsakas, N.; Lehn, J.-M. *Chem. Commun.* **2004**, 62–63. Wu, Z.-Q.; Jiang, X.-K.; Zhu, S.-Z.; Li, Z.-T. *Org. Lett.* **2004**, *6*, 229–232.
18. Berl, V.; Huc, I.; Khoury, R. G.; Lehn, J.-M. *Chem. Eur. J.* **2001**, *7*, 2798–2809. Huc, I.; Maurizot, V.; Gornitzka, H.; Léger, J.-M. *Chem. Commun.* **2002**, 578–579. Dolain, C.; Maurizot, V.; Huc, I. *Angew. Chem., Int. Ed.* **2003**, *42*, 2738–2740.

19. Berl, V.; Huc, I.; Khoury, R. G.; Krische, M. J.; Lehn, J.-M. *Nature* **2000**, *407*, 720–723. Berl, V.; Huc, I.; Khoury, R. G.; Lehn, J.-M. *Chem. Eur. J.* **2001**, *7*, 2810–2820. Maurizot, V.; Léger, J. -M.; Guionneau, P.; Huc, I. *Russ. Chem. Bull.* **2004**, in press.
20. Acocella, A.; Venturini, A.; Zerbetto, F. *J. Am. Chem. Soc.* **2004**, *126*, 2362–2367.
21. Final products were purified by chromatography at least three times on TLC or radial chromatography prior to NMR studies. The impurities can be characterized as such and not as being other conformations/aggregates of the oligomers because: (i) TLC reveals their presence; (ii) the line shape of their signals remains sharp at any temperature even when the rest of the spectrum broadens due to coalescence phenomena; (iii) when the concentration is varied, the proportions of single and double helices varies but the quantity of 'impurity' is proportional to neither of them: it remains proportional to the total concentration of single and double helices.
22. The surface involved in π–π stacking in a double helical dimer is similar to that involved in two stacked single helical monomers. It differs from the surface involved in π–π stacking in two dissociated monomers by twice the cross-section of the helix.
23. Crystal structures show that pyridine rings are sandwiched between amide functions in the single helices, whereas they are sandwiched between other pyridine rings in the double helices, see Ref. 19.
24. Blackburn, G. M., Gait, M. J., Eds.; *Nucleic Acids in Chemistry and Biology*; 2nd ed.; Oxford University Press: Oxford, 1996.